Hybrid Photonic Crystal Fiber Sensing of High Hydrostatic Pressure

Marcos A. R. Franco[a,b], Valdir A. Serrão[b] ,Tânia R. Pitarello[a], Arismar Cerqueira S. Jr.[c]
[a] Instituto Tecnológico de Aeronáutica-ITA, São José dos Campos-SP, 12228-900, Brazil
[b] Instituto de Estudos Avançados – IEAv, São José dos Campos-SP, 12228-900, Brazil
[c] Faculdade de Tecnologia, Universidade Estadual de Campinas – UNICAMP, Limeira-SP, Brazil

ABSTRACT

The opto-mechanical response of Hybrid Photonic Crystal Fiber (HPCF) with Ge-doped inclusions is numerically modeled for high hydrostatic pressure sensing purpose. A typical photonic crystal fiber (PCF) consists of a silica solid-core and a cladding with a hexagonal lattice of air-holes. The HPCF is similar to the regular PCF, but a horizontal line of air-holes is substituted by solid high index rods of Ge-doped silica. The optical guidance in HPCFs is supported combining two physical effects: the modified total internal reflection and the photonic bandgap. In such fibers, the Ge-doped inclusions induce residual birefringence. In our analysis, we evaluate the susceptibility of the phase modal birefringence and group birefringence to hydrostatic pressure. The analyses were performed at a photonic bandgap with central wavelength near to 1350 nm. The polarimetric pressure sensitivity is about 10 rad/MPa x m at λ = 1175 nm.

Keywords: Fiber Optic Sensor, Pressure Sensor, Birefringence, Photonic Bandgap, Photonic Crystal Fiber, Microstructured Optical Fiber

1. INTRODUCTION

Hybrid Photonic Crystal Fiber (HPCF) is a novel type of photonic crystal fiber (PCF) that supports optical guidance by two physical effects: the modified total internal reflection (mTIR) and photonic bandgap (PBG) [1-4]. The HPCF is composed of air-holes and Germanium-doped silica rods disposed around an undoped silica core. The air-holes are arranged in a hexagonal lattice as in index-guiding PCFs, whereas the high-index rods replace a single row of air holes along one of the PCF axes. The Figure 1 shows the geometric design of HPCF, where along y-axis the core has a higher refractive index than the effective refractive index of the cladding, so along this axis light can be guided by the mTIR effect from two half-spaces of microstructured silica. On the other hand, along the x-axis mTIR is not possible, since the cladding rods have a higher index than the core. In this case, confinement only occurs in restricted bands of wavelength (photonic bandgaps).

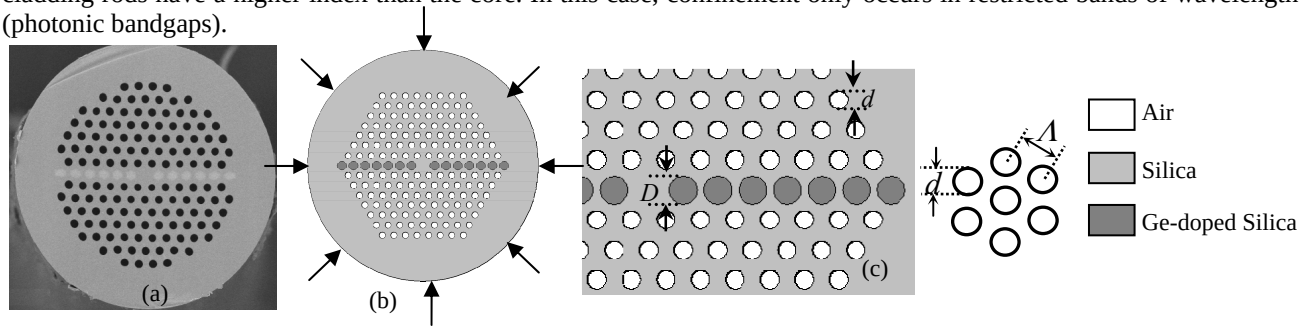

Figure 1. Hybrid photonic crystal fiber design. (a) Fabricated HPCF. (b) HPCF geometric model and applied hydrostatic pressure. (c) Main geometric parameters of the microstructure. The HPCF geometric parameters are: D = 6.38 μm, d = 4.34 μm and Λ = 8 μm.

2. MODELLING METHOD

The numerical analyses were realized by a weakly coupled scheme to model the opto-mechanical response of HPCF. The residual induced stress, caused by the different thermal expansion coefficients of silica and Ge-doped silica, and the mechanical displacements consequence of the hydrostatic applied pressure are considered in the plane strain approximation. From the displacements is possible to determine the distribution of the normal stresses in the cross

This work was partially supported by the CAPES (grant 23038.029912/2008-05), and FINEP (grants 0.1.06.1177.00 and 0.1.05.0770.00).

21st International Conference on Optical Fiber Sensors, edited by Wojtek J. Bock, Jacques Albert, Xiaoyi Bao,
Proc. of SPIE Vol. 7753, 775346 · © 2011 SPIE · CCC code: 0277-786X/11/$18 · doi: 10.1117/12.885961

section of the fiber, and by the elastooptic effect, that couples the mechanical stress to the optical index of refraction, is possible to evaluate the anisotropic profile of refractive indexes in the silica and the Ge-doped regions. From the new refractive indexes profiles we evaluate the optical propagation characteristics by the modal analyses based on the solution of full vectorial Helmholtz equation. In the opto-mechanical coupled analysis it was used a commercial finite element program (COMSOL). To the stress calculations were used Lagrange type finite elements and to the optical modal analyses were used vector finite elements (edge elements). An anisotropic cylindrical Perfectly Matched Layer (PML) was used as the domain truncation technique in the optical analyses.

The analyzed HPCF has high index inclusions of Ge-doped silica that causes residual stress and induced birefringence during the fabrication process. To model the residual stress is necessary to know the mechanical properties of Ge-doped silica that depends of the GeO_2 concentration. In this study we considered Ge-doped rods with parabolic profile of refractive index. The main mechanical and optical properties of Ge-doped silica as function of the GeO_2 concentration are [5-17]:

$$N_{dop} = (1 - X_{mol}) . N_{SiO_2} + X_{mol} . N_{GeO_2} , \tag{1}$$

$$N_{dop}(r) = N_{dop}^{\max} . \left[1 - 2 . \Delta_N (r/a)^2\right]^{1/2}, \quad \text{with} \qquad \Delta_N = \left\{ \left(N_{dop}^{\max}\right)^2 - N_{siO_2}^2 \Big/ 2 . \left(N_{dop}^{\max}\right)^2 \right\} , \tag{2}$$

$$X_{mol}(r) = \left(N_{dop}(r) - N_{SiO_2}\right) \Big/ \left(N_{GeO_2} - N_{SiO_2}\right) , \tag{3}$$

$$\alpha_{dop} = \alpha_{SiO_2} + \alpha_{GeO_2} . X_{mol} , \tag{4}$$

$$\alpha_{dop}(r) = \alpha_{dop}^{\max} . \left[1 - 2 . \Delta_T (r/a)^2\right]^{1/2}, \quad \text{with} \qquad \Delta_T = \left\{ \left(\alpha_{dop}^{\max}\right)^2 - \alpha_{siO_2}^2 \Big/ 2 . \left(\alpha_{dop}^{\max}\right)^2 \right\} , \tag{5}$$

$$T_{ann}^{dop}(r) = T_{ann}^{SiO_2} - 1000 . X_{mol}(r) , \tag{6}$$

$$E_{dop}(r) = (1 - 0.8 . X_{mol}(r)) . E_{SiO_2} , \tag{7}$$

$$\upsilon_{dop}(r) = (1 - 0.50 . X_{mol}(r)) . \upsilon_{SiO_2} , \tag{8}$$

where N represent the refractive index to the materials SiO_2 or GeO_2, N_{SiO2} is evaluated by the Sellmeier equation, N_{dop} is the refractive index of Ge-doped silica, $N_{dop}^{\max} = 1.023\, N_{SiO_2}$, X_{mol} is the molar fraction of GeO_2, α_{SiO2}=5.5 10^{-7} and α_{GeO2}=1.04 10^{-5} are the thermal expansion coefficients of silica and GeO_2, T_{ann} is the annealing point, $T_{ann}^{SiO_2} = 1130\ ^oC$, E is the Young´s module, E_{SiO2} = 72.5 GPa and E_{GeO2} = 43.3 GPa, υ is the Poisson ratio, υ_{SiO2} = 0.165 and υ_{GeO2} = 0.197.

Taken into account the elastooptic effect is possible to represent the refractive index changed by the stresses as:

$$N_1 = N + C_1\,\sigma_1 + C_2(\sigma_2 - \sigma_3), \quad N_2 = N + C_1\,\sigma_2 + C_2(\sigma_1 - \sigma_3), \quad N_3 = N + C_1\,\sigma_3 + C_2(\sigma_1 - \sigma_2), \tag{9}$$

where N is the refractive index of not stressed material (silica or Ge-doped silica), C_1 and C_2 are the stress-optic coefficients and σ_1 σ_2 and σ_3 are the principal components of the induced stress. For PCFs, considering the uniformity of the glass composition, the axial stress $\sigma_3 = 0$. The principal stress components can be evaluated by $\sigma_{1,2} = 0.5 \left\{ (\sigma_x + \sigma_y) \pm \left[(\sigma_x - \sigma_y)^2 + 4\,\tau_{x,y}^2 \right]^{1/2} \right\}$, however the contribution of shear stress $\tau_{x,y}$ is relatively small in the core region and its neighborhood and it will be neglected in this work ($N_1 \equiv N_x$, $N_2 \equiv N_y$, and $N_3 \equiv N_z$).

The residual stress and the applied hydrostatic pressure change the isotropic materials to non-homogeneous anisotropic materials leading to a material birefringence distribution. As a consequence of material birefringence, the two linearly polarized fundamental optical modes (FM_x and FM_y) present phase birefringence (B_p). The material birefringence, the phase birefringence, and the group birefringence (B_g) can be defined by:

$$B_m = (C_1 - C_2) . (\sigma_x - \sigma_y), \qquad B_p = n_{eff_X} - n_{eff_Y} , \qquad B_g = B_p - \lambda \left(dB_p / d\lambda\right), \tag{11}$$

where n_{eff} is the effective index of fundamental optical modes.

3. RESULTS

The Figures 2(a) and 2(b) present the material birefringence, induced by residual stress and applied pressure, near the fiber's core in the x and y-axis, respectively. Figures 2(c)-2(d) show the material birefringence induced by the residual stress (P = 0 bar) and induced by both the residual stress and the hydrostatic applied pressure (P = 500 bar), respectively. The effect of applying hydrostatic pressure is to decrease B_m in x direction, but in the y-axis the pattern of B_m is modified increasing its value in the center core and decreasing near the space between two air-holes above and below the core. The differential effect of pressure over B_m will affect differently the FM_x and FM_y modes.

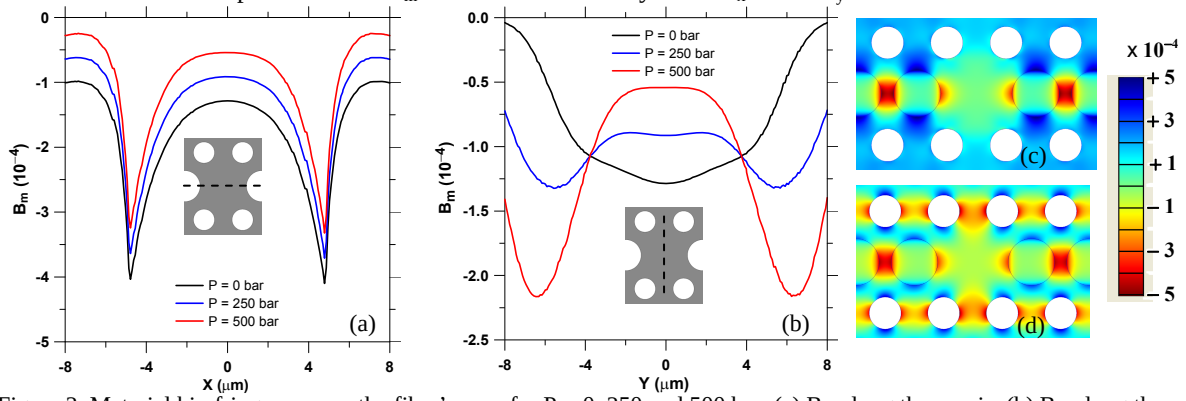

Figure 2. Material birefringence near the fiber's core for P = 0, 250 and 500 bar. (a) B_m along the x-axis. (b) B_m along the y-axis.

The Figure 3(a) presents the spectral transmission at the bandgap with central wavelength ~1350 nm and n_{eff} for both FM_x and FM_y modes. The Figure 3(b) shows the confinement losses at the left edge of bandgap for P = 0 and 500 bar. Figure 3(c) presents a typical distribution of modal optical energy in the HPCF. Without applied pressure the HPCF has a polarimetric extinction ratio (PER) of about 50 dB at λ = 1160 nm, useful for single mode single polarization applications. The bandgap position can be shifted adjusting the Ge-doped rods diameters [4]. Appling hydrostatic pressure (500 bar) leads to drastically decrease the polarimetric extinction ratio from 50 dB to about 15 dB at 1160 nm.

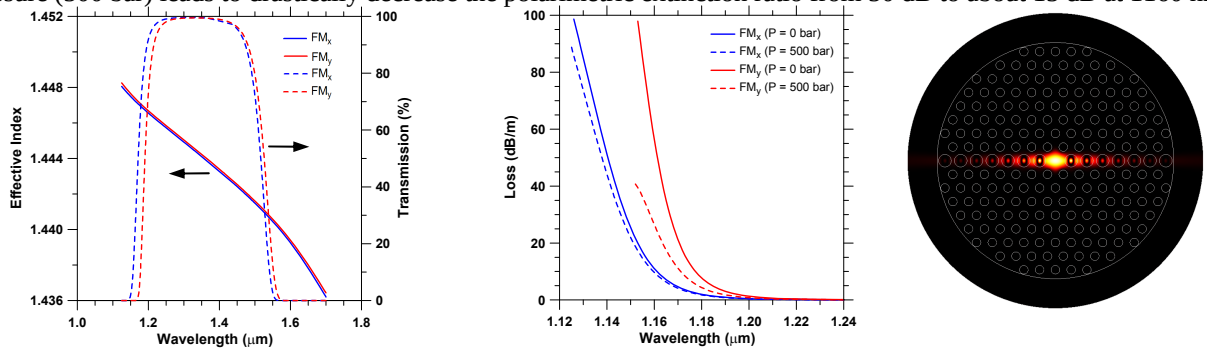

Figure 3. (a) Effective index of FM_x and FM_y modes and respective spectral transmission without applied pressure. (b) Confinement losses of fundamental modes near the left edge of bandgap considering P = 0 and 500 bar. (c) Typical modal energy distribution of fundamental guided mode in HPCF.

Figure 4(a) presents the phase and group birefringence across the entire bandgap for P = 0 bar. Figure 4(b) shows the B_p and B_g near the left edge of bandgap for P = 0 and 500 bar, and Figure 4(c) presents the susceptibility of phase and group birefringences (dB_p/dP) and (dB_g/dP) to hydrostatic pressure near the left edge of the bandgap. B_p and B_g vary quickly in the bandgap edge and is almost constant in the center of the bandgap. The rapid variation in B_p and B_g allows to use it as a sensing parameter. The maximum susceptibility of B_p and B_g were $dB_p/dP=1.10^{-6}$ (at λ=1135 nm) and $dB_g/dP=7.10^{-6}$ (at λ=1175 nm), respectively.

4. CONCLUSION

For the first time the opto-mechanical response of a hybrid photonic crystal fiber was numerically investigated for hydrostatic pressure sensor application. The HPCF has a high polarimetric extinction ratio of ~50 dB that is reduced to ~15 dB at λ = 1160 nm when submitted to hydrostatic pressure variation of 500 bar, this effect can also be used as a sensing parameter. On the other hand, the phase and group birefringences vary quickly at the edge of photonic bandgaps

and demonstrate the potential of HPCF as a pressure element sensor. The non-optimized HPCF design allows reaching a phase and grouping susceptibility to hydrostatic pressure of: $dB_p/dP=1.10^{-6}$ (at λ=1135 nm) and $dB_g/dP=7.10^{-6}$ (at λ=1175 nm), respectively.

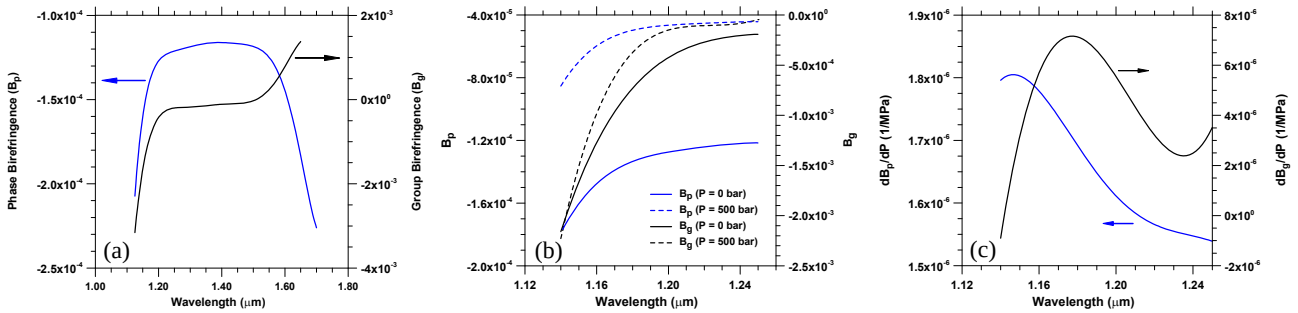

Figure 4. Phase and group birefringence, and the susceptibility of phase and group birefringence to hydrostatic pressure. (a) Phase and group birefringence in entire bandgap without pressure (P = 0 bar). (b) Phase and group birefringence at the left edge of the bandgap considering hydrostatic pressure of 0 bar and 500 bar. (c) Susceptibility of phase and group birefringence at the left edge of the bandgap (ΔP = 500 bar).

REFERENCES

1. Cerqueira A. S., *et al*, "Hybrid photonic crystal fiber," Opt. Express 14, N. 2, 926-931 (2006).
2. Cerqueira, A. S., "Recent progress and novel applications of photonic crystal fibers," Rep. Prog. Phys., 73, 023301 (2010).
3. Cerqueira A. S., *et al*, "Birefringence properties of hybrid photonic crystal fibers," proceedings of Microwave and optoelectronics Conference (IMOC 2009), 804-806, Belem, Brazil, 03-06, November, (2009).
4. Franco, M. A. R., *et al*, "Thermal tunability of photonic bandgaps in photonic crystal fibers selectively filled with nematic liquid crystal," Proceedings of 2nd Workshop on Specialty Optical Fibers and Their Applications (WSOF-2), Oaxaca, Mexico, 13-15, October, (2010).
5. Fleming, J. W., "Dispersion in GeO2 -SiO2 glasses," Appl. Opt. 23(24), 4486-4493 (1984).
6. Martynkien, T., *et al*., "Highly birefringent microstructured fibers with enhanced sensitivity to hydrostatic pressure," Opt. Express 18(14), 15113-15121 (2010).
7. Kühn, B. and Schadrack, R., "Thermal expansion of synthetic fused silica as a function of OH content and fictive temperature," J. Non-Cryst. Solids 355, 323-326 (2009).
8. Gupta, D., Kumar, A., Thyagarajan, K., "Polarization mode dispersion in single mode optical fibers due to core-ellipticity," Opt. Commun. 263, 36-41 (2006).
9. Koshiba, M., [Optical Waveguide Theory by the Finite Element Method], KTK Scientific Publishers and Kluwer Academic Publishers, Tokyo, 133-160 (1992).
10. Urbanczyk, W., Martynkien, T., Bock, W. J., "Dispersion effects in elliptical-core highly birefringent fibers," Appl. Opt. 40(12), 1911-1920 (2001).
11. Olszewski, J., "Birefringence analysis in photonic crystal fibers with germanium-doped core," J. Opt. A: Pure Appl. Opt. 11, 1-10 (2009).
12. Martynkien, T., Urbanczyk, W., "Modeling of spectral characteristics of Corning PMF-38 highly birefringent fiber," Optik 113(1), 25-30 (2002).
13. Hlubina, P., *et al*., "Broad spectral range measurements and modelling of birefringence dispersion in two-mode elliptical-core fibres," J. Opt. 12, 1-8 (2010).
14. Martynkien, T., *et al*., "Birefringence in microstructure fiber with elliptical GeO_2 highly doped inclusion in the core," Opt. Lett. 33(23), 2764-2766 (2008).
15. Verbandt, Y., *et al*., "Polarimetric Optical Fiber Sensors: Aspects of Sensitivity and Practical Implementation," Opt. Rev. 4(1A), 75-79 (1997).
16. Lagakos, N., Bucaro, J. A., Hughes, R., "Acoustic sensitivity predictions of single-mode optical fibers using Brillouin scattering," Appl. Opt. 19(21), 3668-3670 (1980).
17. Chiang, K., S., Sceats, M., G., Wong, D., "Ultraviolet photolytic-induced changes in optical fibers: the thermal expansion coefficient," Opt. Lett. 18(12), 965-967 (1993).

E-mail: marcos@ieav.cta.br; phone +55 12 3947-5522